Audio Engineering Society

Convention Paper 10618

Presented at the 153rd Convention
2022 October

Piezoelectric Actuators for Flat-Panel Loudspeakers

Michael C. Heilemann and Tre DiPassio

University of Rochester, Rochester, NY, USA

Correspondence should be addressed to Michael C. Heilemann (mheilema@ur.rochester.edu)

ABSTRACT

Piezoelectric actuators offer advantages in terms of weight and form-factor when compared with traditional inertial exciters used to drive flat-panel loudspeakers. Unlike inertial exciters, piezoelectric actuators induce vibrations in the panel by generating bending moments at the actuator edges. Models for piezoelectric excitation are developed, and it is shown that piezoelectric actuators are most effective at driving resonant modes whose bending half-wavelength is the same size as the actuator dimensions, giving a natural boost to the high-frequency response. Flat-panel loudspeaker design techniques such as the modal crossover method, and the corresponding array layout optimization are adapted using the model for the response of piezo-driven panels. The adapted design techniques are shown to eliminate the isolated, low-frequency bending modes responsible for reduced sound quality on a prototype panel speaker.

1 INTRODUCTION

Flat-panel loudspeakers traditionally radiate sound by employing one or more inertial exciters fixed to the panel to drive bending waves on the surface [1, 2, 3, 4, 5, 6]. Inertial exciters are widely available commercially, and their designs (similar to those of conventional loudspeaker drivers) generally consist of a permanent magnet, suspension, and voice coil. However, inertial exciters may present design issues in small, portable electronic devices such as smartphones [7] that require a transparent screen or a compact form-factor.

Piezoelectric actuators offer an alternative form of excitation. Physically, they are thin and lightweight compared to inertial drivers, making them useful for compact flat-panel loudspeaker designs. A number of studies have shown piezoelectric actuators to be an effective means of inducing bending vibrations in beams and plates for active vibration control [8, 9, 10, 11, 12]. Though some works have explored the use of piezoelectric actuators to radiate sound from panel-like structures such as vehicle doors [13, 14] using a single actuating element, the low-frequency performance of these speakers is limited by poor coupling between the actuator and panel bending waves at these frequencies. For this reason, piezo-driven speakers are typically small devices that focus on audio reproduction above 250 Hz – 300 Hz [7, 15, 16, 17].

Actuator arrays have demonstrated effectiveness in improving the low-frequency response of flat-panel speakers by allowing the designer to selectively drive bending modes that have desirable sound radiation properties. A crossover network [18] may be employed so that at low-frequencies, the actuator array drives the fundamental mode of the panel while canceling the contributions of the other modes that resonate within the array bandwidth. At high-frequencies, sufficiently

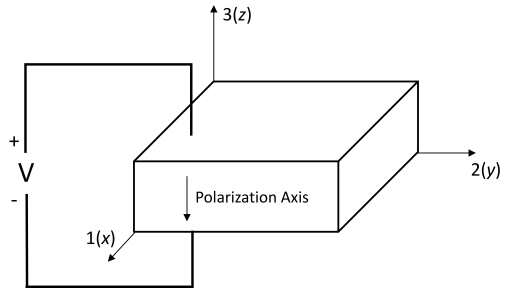

Fig. 1: Coordinate system for a piezoelectric actuator polarized in the z direction.

damped panels can achieve a relatively flat frequency response due to high modal overlap [19, 20]. In this work, we model the vibrational response of a panel loudspeaker excited by one or more piezoelectric actuators. An adaptation to an array layout optimization [21] for modal crossover networks is developed using the model for piezo-driven panels, and design guidelines are suggested for piezo-driven panel speakers.

2 THEORETICAL DEVELOPMENT

The lumped element model presented in this section describing the vibrational response of a panel driven by a piezoelectric actuator follows from early work by Crawley and de Luis [8] who demonstrated that piezoelectric actuators are effective in controlling vibrations in beams. Their analysis uses actuators polarized in the z direction, meaning that the actuator will expand or contract in the x and y directions depending on the polarity of the voltage applied across the z dimension as shown in Fig. 1.

Inertial effects of the piezoelectric element can be ignored as long as the piezoelectric element is thin and lightweight compared to the panel [22], though these effects have been explored in other works [23]. When a voltage V is applied across the polarization direction of an unconstrained actuator, the actuator will experience strains ε_{pe}^1 and ε_{pe}^2 in the 1 and 2 directions respectively given by,

$$\varepsilon_{pe}^1 = \frac{d_{31}V}{h_{pe}}, \qquad \varepsilon_{pe}^2 = \frac{d_{32}V}{h_{pe}}, \tag{1}$$

where h_{pe} is the piezoelectric actuator thickness, and d is the piezoelectric strain constant. The subscript indices 31 and 32 refer to the direction of the applied voltage (3), and the direction of displacement (1 or 2) respectively.

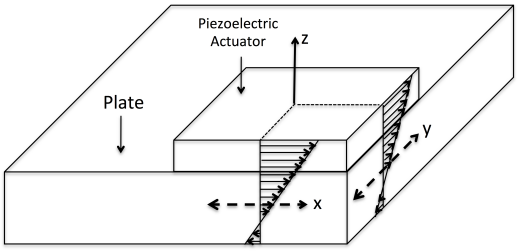

Fig. 2: Strain distribution induced by a piezoelectric actuator perfectly bonded to one side of a panel. Reproduced from [26].

2.1 Modeling Induced Strain

Following [24] and [25], an applied voltage across an actuator perfectly bonded to the panel surface will cause the panel to bend and stretch, leading to an asymmetric strain distribution as shown in Fig. 2. The strain distribution $\varepsilon(z)$ may be modeled as,

$$\varepsilon(z) = Cz + \varepsilon_0, \tag{2}$$

where, C is the slope, and ε_0 is the z intercept. It is assumed that the actuator has similar properties in the 1 and 2 dimensions so that $d_{31} = d_{32}$.

Following [25] the asymmetric strain distribution may be modeled as the superposition of a symmetric distribution (resulting in pure bending) and a uniform strain distribution (resulting in pure longitudinal motion), inducing both longitudinal and bending waves in the panel. It is important to note that applications such as active vibration control require specific relative excitations of both bending and longitudinal waves [27]. For this reason, actuators may be symmetrically aligned on opposite sides of the structure, so that their relative phases may be adjusted to drive the specified wave forms. For example, driving the two actuators in phase will give pure longitudinal motion, and driving the two actuators 180° out of phase will give pure bending motion. Though the aligned pair of actuators is better suited than a single actuator to efficiently drive sound producing bending waves for flat-panel loudspeakers, the configuration is not conducive to panel speakers on thin electronic devices such as smartphones, where the actuator would be visible on the screen.

Combining (2) with Hooke's Law gives the stresses in the panel σ_p and the actuator σ_{pe} as,

$$\sigma_p(z) = \frac{E_p}{1-\nu_p}(Cz + \varepsilon_0), \tag{3}$$

and

$$\sigma_{pe}(z) = \frac{E_{pe}}{1-\nu_{pe}}(Cz + \varepsilon_0 - \varepsilon_{pe}), \tag{4}$$

Where E is the Young's modulus, and ν is the Poisson's ratio, noting that the subscripts p and pe refer to properties of the panel and the piezoelectric actuator respectively.

The constants C and ε_0 may be determined by applying moment equilibrium about the x or y axis,

$$\int_{-h_p}^{h_p} \sigma_p(z) z dz + \int_{h_p}^{h_p+h_{pe}} \sigma_{pe}(z) z dz = 0, \tag{5}$$

and force equilibrium in the x or y direction,

$$\int_{-h_p}^{h_p} \sigma_p(z) dz + \int_{h_p}^{h_p+h_{pe}} \sigma_{pe}(z) dz = 0, \tag{6}$$

where h_p is the half-thickness of the plate.

Solving (5) and (6) gives,

$$C = K^b \varepsilon_{pe}, \tag{7}$$

and

$$\varepsilon_0 = K^l \varepsilon_{pe}, \tag{8}$$

The material geometric constants K^b and K^l are given by,

$$K^b = \frac{12E_{pe}E_p h_p(h_{pe}^2 + 2h_p h_{pe})}{16E_p^2 h_p^4 \frac{(1-\nu_{pe})}{(1-\nu_p)} + \beta + E_{pe}^2 h_{pe}^4 \frac{(1-\nu_p)}{(1-\nu_{pe})}}, \tag{9}$$

$$K^l = \frac{E_{pe}h_{pe}[E_{pe}h_{pe}^3 \frac{(1-\nu_p)}{(1-\nu_{pe})} + 8E_p h_p^3]}{16E_p^2 h_p^4 \frac{(1-\nu_{pe})}{(1-\nu_p)} + \beta + E_{pe}^2 h_{pe}^4 \frac{(1-\nu_p)}{(1-\nu_{pe})}}, \tag{10}$$

where,

$$\beta = E_p E_{pe}[8h_{pe}^3 h_p + 24h_{pe}^2 h_p^2 + 32h_{pe}h_p^3]. \tag{11}$$

One important result from (9) is that the induced flexural strain is maximized when the piezoelectric actuator has the same Young's modulus as the panel. Using a piezoelectric actuator that is either much stiffer, or much more flexible than the panel material will give less efficient force coupling.

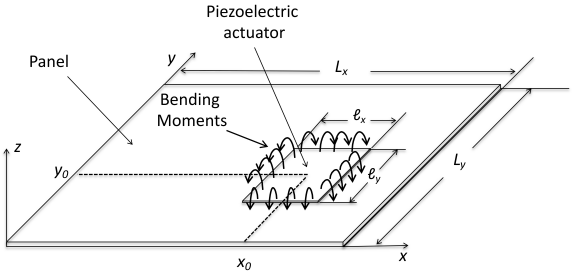

Fig. 3: Bending moments induced in a panel by a piezoelectric actuator of dimensions (ℓ_x, ℓ_y) centered at location (x_0, y_0).

2.2 Response of Simply Supported Plate

Following [28] and [29], the equation of bending motion for a thin, isotropic panel is given by,

$$D\nabla^4 u(x,y,t) + 2\rho h_p \ddot{u}(x,y,t) + b\dot{u}(x,y,t) = P(x,y,t), \tag{12}$$

where $u(x,y,t)$ is the out-of-plane displacement of the panel, ρ is the density of the panel, b is the damping coefficient, and D is the bending stiffness of the panel given by,

$$D = \frac{2E_p h_p^3}{3(1-\nu_p^2)}. \tag{13}$$

From [8], the internal moments M_x and M_y induced in the panel by the piezoelectric actuator are only present in the area covered by the actuator. Following [22], for an actuator of dimensions (ℓ_x, ℓ_y) centered at location (x_0, y_0) on the panel as shown in Fig. 3, these moments may be modeled using unit step functions as,

$$M_x = M_y = DK^b \varepsilon_{pe} \left\{ U\left[x - \left(x_0 - \frac{\ell_x}{2}\right)\right] - U\left[x - \left(x_0 + \frac{\ell_x}{2}\right)\right] \right\} \left\{ U\left[y - \left(y_0 - \frac{\ell_y}{2}\right)\right] - U\left[y - \left(y_0 + \frac{\ell_y}{2}\right)\right] \right\}. \tag{14}$$

The external pressure on the panel may be expressed in terms of the bending moments as,

$$p(x,y,t) = \frac{\partial^2 M_x}{\partial^2 x} + \frac{\partial^2 M_y}{\partial^2 y}. \tag{15}$$

The response of the panel $u(x,y,t)$ may be expressed as a superposition of modes given by,

$$u(x,y,t) = \sum_{r=1}^{\infty} \alpha_r \Phi_r(x,y) e^{j\omega t}, \tag{16}$$

where α_r and $\phi_r(x,y)$ are the amplitudes and spatial responses of each mode at frequency ω. Assuming the panel is rectangular with simply supported edges, the spatial response of each mode is sinusoidal,

$$\Phi_r(x,y) = \sin\left(\frac{m_r\pi}{L_x}x\right)\sin\left(\frac{n_r\pi}{L_y}y\right), \qquad (17)$$

where m_r and n_r indicate the number of half-wavelengths in the horizontal and vertical dimensions respectively. Combining (12) and (14-17), and solving for α_r gives,

$$\alpha_r = \frac{4F_r^{eq}\Phi_r(x_0,y_0)}{\rho h_p L_x L_y(\omega_r^2 - \omega^2 + \frac{j\omega_r\omega}{Q_r})}, \qquad (18)$$

where Q_r is the quality factor of each mode, ω_r is the resonant frequency of each mode, and F_r^{eq} is the equivalent force on each mode given by,

$$F_r^{eq} = -4DK^b\varepsilon_{pe}\left[\frac{m_r^2L_y^2 + n_r^2L_y^2}{m_r n_r L_x L_y}\right]\Phi_r(\frac{\ell_x}{2},\frac{\ell_y}{2}). \qquad (19)$$

As with conventional inertial exciters, the force exerted on a particular mode is determined by the coupling between the location of the actuator relative to the nodal lines of the mode. Actuators located in the antinodal region of a mode will have strong coupling to the mode, while actuators located on nodal lines of a mode will not be able to excite that mode. Since piezoelectric actuators excite the panel by bending, the excitation of each mode is also dependent on the size of the actuator relative to the wavelength of the mode it is trying to excite as shown in (19). For this reason, small actuators have relatively poor coupling to the lowest resonant modes, producing an acoustic response where high-frequencies are boosted relative to low-frequencies.

It should be noted that though the longitudinal waves induced in the panel by the single-piezo setup are not inherently sound-producing, they may be converted into sound-producing bending waves at discontinuities such as the boundaries of the panel [25]. However, since panels are much stiffer in extension than bending, small actuators will have weaker coupling to longitudinal waves than bending waves. For this reason, longitudinal effects will be ignored at low frequency when the actuator is small compared to the longitudinal wavelength [26]. Wave conversion effects may be further reduced by losses due to edge damping.

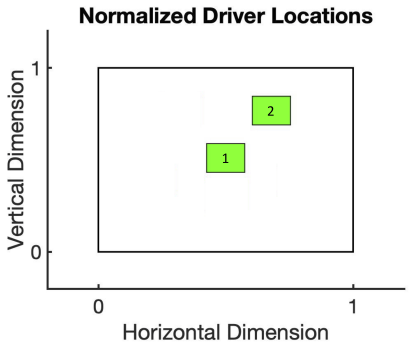

Fig. 4: Locations of two piezoelectric actuators used for the simulations shown in Figs. 5 and 6, where actuator 1 is centered at the normalized location (0.5,0.51), and actuator 2 is centered at the normalized location (0.68, 0.77).

3 EVALUATION OF MODEL

The model was tested on a 304 mm × 203 mm × 0.9 mm glass panel using rectangular piezoelectric actuators made of Navy Type II material with dimensions of 45.7 mm × 31.7 mm × 0.23 mm. The properties for the glass and piezoelectric actuator are shown in Table 1.

Table 1: Glass and piezoelectric material properties

	E [GPa]	ν	ρ [kg m^{-3}]	d_{31} [m V^{-1}]
Glass	72	0.23	2520	N/A
Piezo [30]	52	0.34	7800	-190×10^{-12}

The resonant frequencies of the panel modes were estimated for the simulation using an approximation for the resonant frequencies of panels with clamped boundary conditions [31]. Each mode in the simulation was assumed to have a quality factor of 30. The locations for the piezoelectric actuators are shown in Fig. 4, where actuator 1 is centered at the normalized location (0.5,0.51), and actuator 2 is centered at the normalized location (0.68, 0.77). The average acceleration of the panel is shown for the two actuator locations in Figs. 5 and 6 respectively. The measured response is the average acceleration of the panel acquired using a Polytec PSV 500 scanning laser vibrometer. The response predicted by the model has a strong agreement with the measured response.

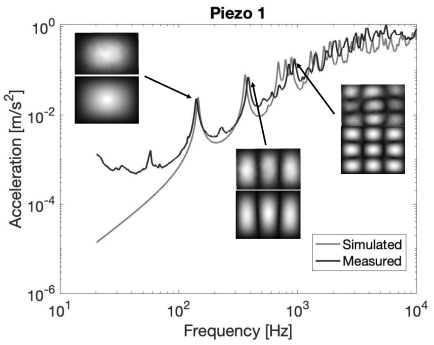

Fig. 5: Simulated and measured response of a glass panel driven by a piezoelectric actuator centered at location 1 in Fig. 4. The simulated and measured responses of the panel surface are shown in the top and bottom viewgraphs respectively at select frequencies.

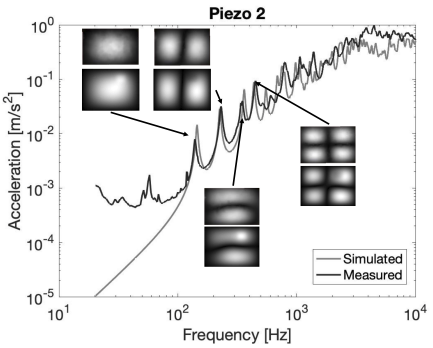

Fig. 6: Simulated and measured response of a glass panel driven by a piezoelectric actuator centered at location 2 in Fig. 4. The simulated and measured responses of the panel surface are shown in the top and bottom viewgraphs respectively at select frequencies.

3.1 High-Frequency Equalization

From (19), the force induced in the panel by a piezoelectric actuator is dependent on the size of the actuator relative to the modal wavelength. When the dimensions of the actuator are small relative to the dimensions of the panel, the actuator will impart a stronger force on high-frequency modes than low-frequency modes. This effect is evident in both Figs. 5 and 6, where the acceleration of the panel increases with frequency. The panel acceleration $\ddot{u}(x,y,t)$ is related to the radiated sound pressure at a point (x_s,y_s,z_s) in space via the Rayleigh integral [32],

$$p(x_s,y_s,z_s,t) = \frac{\rho_0}{2\pi}\iint_S \frac{\ddot{u}(x,y,t-R/c)}{R}ds, \qquad (20)$$

$$R = \sqrt{(x_s-x)^2+(y_s-y)^2+z_s^2} \qquad , \qquad (21)$$

where ρ_0 is the density of air, c is the speed of sound in air, and R is the distance from a point on the panel (x,y) to a point in space (x_s,y_s,z_s)

Conventional equalization may be employed to balance the high-frequency signal level. Boosting the bass response using equalization alone may introduce nonlinearities in the signal chain. Note that the material properties and/or dimensions of the panel may be adjusted to further extend the low-frequency response.

4 PIEZOELECTRIC ACTUATOR ARRAYS

Actuator arrays may be employed to boost the low-frequency response and cancel vibration modes that have adverse radiation qualities. The array may be used as part of a modal crossover network [18] to drive the low-frequency response of the loudspeaker, while the high-frequencies are reproduced through a single actuator. From (18) the amount of force exerted by an actuator on a particular mode is dependent on the actuator's location relative to the nodal lines of the mode. When more than one actuator is involved, the total force on each mode is given as the sum of the forces due to each actuator individually. For an array of N actuators at locations (x_i,y_i) each exerting a force d_i, the force f_r on the r$^{\text{th}}$ mode is given by,

$$f_r = \sum_{i=1}^{N} d_i \Phi_r(x_i,y_i). \qquad (22)$$

This can be expressed in matrix form as,

$$\mathbf{F} = \mathbf{G}\mathbf{D}, \qquad (23)$$

where $\mathbf{F}$ is a vector of mode forces for a set of M modes, $\mathbf{G}$ is a matrix of coupling factors and $\mathbf{D}$ is a vector of actuator forces.

$$\mathbf{F} = \begin{bmatrix} f_{r=1} \\ f_2 \\ \vdots \\ f_{r=M} \end{bmatrix} \qquad \mathbf{D} = \begin{bmatrix} d_{i=1} \\ d_2 \\ \vdots \\ d_{i=N} \end{bmatrix} \qquad (24)$$

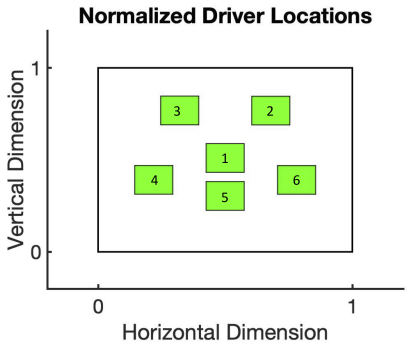

Fig. 7: Optimized layout for an array of six piezoelectric actuators exciting the panel described in the previous example. The normalized center locations of each actuator are given in Table 2.

$$\mathbf{G} = \begin{bmatrix} \Phi_{r=1}(x_{i=1},y_{i=1}) & \Phi_1(x_2,y_2) & \cdots & \Phi_1(x_N,y_N) \\ \Phi_2(x_1,y_1) & \Phi_2(x_2,y_2) & \cdots & \Phi_2(x_N,y_N) \\ \vdots & \vdots & \vdots & \vdots \\ \Phi_M(x_1,y_1) & \Phi_M(x_2,y_2) & \cdots & \Phi_{r=M}(x_{i=N},y_{i=N}) \end{bmatrix} \quad (25)$$

It is convenient for the actuator array elements to be positioned so they can excite the desired modal response while being driven by a common source signal. For use in a modal crossover network, the array is configured to drive the fundamental mode of a panel, while simultaneously cancelling the contributions of as many other modes as possible. For N identical point-force exciters, (24) may be expressed ideally as,

$$\mathbf{F} = \begin{bmatrix} f_{r=1} \\ 0 \\ \vdots \\ 0 \end{bmatrix} \qquad \mathbf{D} = \begin{bmatrix} 1 \\ 1 \\ \vdots \\ 1 \end{bmatrix} \quad (26)$$

Following [21], the locations of the actuators may be optimized to maximize the force on mode $r = 1$ and minimize the forces on modes $r = 2$ through $r = M$.

$$\underset{(x_i,y_i)}{\operatorname{argmin}} \sqrt{\frac{1+\sum_{r=2}^{M} f_r}{f_1}} \quad (27)$$

Since the force exerted by a piezoelectric actuator on a particular mode is determined by both the size of the actuator and the dimensions of the actuator, the equations must be modified to account for the additional coupling factor. Equation (25) may be expressed as,

Table 2: Normalized center locations of an optimized array of six piezoelectric actuators. The layout is shown in Fig. 7.

Actuator	x	y
1	0.50	0.51
2	0.68	0.77
3	0.32	0.77
4	0.22	0.39
5	0.50	0.30
6	0.78	0.39

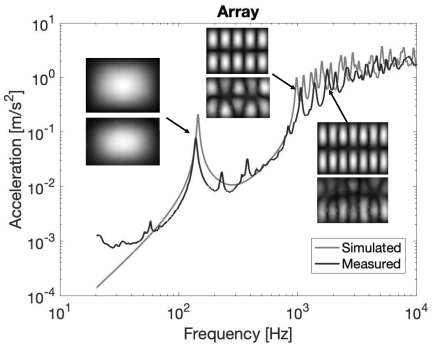

Fig. 8: Simulated and measured response of a glass panel driven by an array of piezoelectric actuator centered at the locations given in Table 2. The simulated and measured responses of the panel surface are shown in the top and bottom viewgraphs respectively at select frequencies.

$$\mathbf{G} = \begin{bmatrix} \Gamma_1\Phi_1(x_1,y_1)\Phi_1(\frac{\ell_{x_1}}{2},\frac{\ell_{y_1}}{2}) & \cdots & \Gamma_1\Phi_1(x_N,y_N)\Phi_1(\frac{\ell_{x_N}}{2},\frac{\ell_{y_N}}{2}) \\ \Gamma_2\Phi_2(x_1,y_1)\Phi_2(\frac{\ell_{x_1}}{2},\frac{\ell_{y_1}}{2}) & \cdots & \Gamma_2\Phi_2(x_N,y_N)\Phi_2(\frac{\ell_{x_N}}{2},\frac{\ell_{y_N}}{2}) \\ \vdots & \vdots & \vdots \\ \Gamma_M\Phi_M(x_1,y_1)\Phi_M(\frac{\ell_{x_1}}{2},\frac{\ell_{y_1}}{2}) & \cdots & \Gamma_M\Phi_M(x_N,y_N)\Phi_M(\frac{\ell_{x_N}}{2},\frac{\ell_{y_N}}{2}) \end{bmatrix}, \quad (28)$$

where,

$$\Gamma_r = \left[\frac{m_r^2 L_y^2 + n_r^2 L_y^2}{m_r n_r L_x L_y} \right] \quad (29)$$

An example of the optimized array layout is shown in Fig. 7 for an array of six piezoelectric actuators. The properties of the actuators and the panel are the same as those described in the previous example. The center location of each actuator is given in Table 2 normalized to the dimensions of the panel.

The measured and simulated response of the panel when excited by the actuator array is shown in Fig. 8.

The simulated response agrees with the measured data, and the optimized array effectively cancels the contributions of a number of low-frequency resonant modes that appeared in the single-actuator responses shown in Figs. 5 and 6.

It should be noted that if two piezo elements of different material are used in the array, (28) may be modified in a similar way to account for the different relative strains induced by each actuator. As long as all of the piezoelectric actuators are of the same dimensions and material properties, the array layout determined by the optimization routine will be the same as layout used for point force actuators [21].

5 CONCLUSION

While inertial exciters have long been used to excite flat-panel speakers, they can take up a considerable amount of space behind the panel. In devices such as smart phones and tablets, where space inside the device is limited, an alternative form of excitation may be needed to meet the required form-factor. Piezoelectric actuators are very thin compared to commercially available inertial exciters, and may be bonded directly to the rear of a panel. This work provides a first step in modeling the response of piezo-driven panel loudspeakers, and adapting flat-panel loudspeaker design techniques such as the modal crossover network array to work with bending actuators.

Panel loudspeakers excited by piezoelectric actuators typically have a weaker bass response due to the relatively weak coupling between the dimensions of the actuator and the half-wavelength of the fundamental bending mode of the panel. However, in small devices such as smartphones, this fundamental half-wavelength could be much shorter and allow for stronger actuator/panel coupling without incurring additional costs associated with manufacturing large piezoelectric actuators. Since piezoelectric actuators have very strong coupling to high-frequency modes, they may be best used as tweeters in a two-way modal crossover flat-panel speaker, where the low frequencies are reproduced through an array of inertial actuators, and the high-frequencies are reproduced through a single piezoelectric actuator.

6 ACKNOWLEDGMENT

This work was supported by the UR Ventures Technology Development Fund.

References

[1] Bertagni, J., “Flat diaphragm for sound transducers and method for manufacturing it,” 1971.

[2] Bertagni, J., “Flat Diaphragm for Sound Transducers,” 1973.

[3] Bertagni, J., “Flat Loudspeaker with Enhanced Low Frequency,” 1973.

[4] Bertagni, J., “Planar Diaphragm,” 1977.

[5] Azima, H., Colloms, M., and Harris, N., “Panel-Form Loudspeakers,” 2000.

[6] Azima, H., Colloms, M., and Harris, N., “Inertial Vibration Transducer,” 2001.

[7] Kim, T.-H. and Park, G.-C., “Display Device,” 2019, US 2019/0163234A1.

[8] Crawley, E. F. and De Luis, J., “Use of piezoelectric actuators as elements of intelligent structures,” *AIAA Journal*, 25(10), pp. 1373–1385, 1987, doi:https://doi.org/10.2514/3.9792.

[9] Clark, R. L., Flemming, M. R., and Fuller, C. R., “Piezoelectric Actuators for Distributed Vibration Excitation of Thin Plates: A Comparison Between Theory Experiment,” *J. Vib. Acoust.*, 115(3), pp. 332–339, 1993, doi:http://dx.doi.org/10.1115/1.2930353.

[10] Clark, R. L. and Fuller, C. R., “Experiments on active control of structurally radiated sound using multiple piezoceramic actuators,” *J. Acoust. Soc. Am.*, 91(6), pp. 3313–3320, 1992, doi:https://doi.org/10.1121/1.402821.

[11] Clark, R. L., Fuller, C. R., and Wicks, A., “Characterization of multiple piezoelectric actuators for structural excitation,” *J. Acoust. Soc. Am.*, 90(1), pp. 346–357, 1991, doi:https://doi.org/10.1121/1.401257.

[12] Wang, B., Fuller, C. R., and Dimitriadis, E. K., “Active control of noise transmission through rectangular plates using multiple piezoelectric or point force actuators,” *J. Acoust. Soc. Am.*, 90(5), pp. 2820–2830, 1991, doi:https://doi.org/10.1121/1.401879.

[13] Bolzmacher, C., Benbara, N., Rebillat, M., and Mechbal, N., "Piezoelectric Transducer for Low Frequency Sound Generation on Surface Loudspeakers," in *IX ECCOMAS Thematic Conference on Smart Structures and Materials*, pp. 1–10, 2019.

[14] Zenker, B., Dannemann, M., Geller, S., Holeczek, K., Weißenborn, O., Altinsoy, M. E., and Modler, N., "Structure-Integrated Loudspeaker Using Fiber-Reinforced Plastics and Piezoelectric Transducers—Design, Manufacturing and Validation," *Applied Sciences*, 10(10), 2020, doi: https://doi.org/10.3390/app10103438.

[15] Huang, S., Yang, Y., Liu, S., and Chu, X., "A large-diaphragm piezoelectric panel loudspeaker and its acoustic frequency response simulation method," *Applied Acoustics*, 125, pp. 176–183, 2017, doi:https://doi.org/10.1016/j.apacoust.2017.04.003.

[16] Fukuoka, S., Kushima, N., Kawamura, H., and Ninomiya, H., "Acoustic generator," 2014, US 8,897,473 B2.

[17] Anderson, D., "Introduction to modeling and analysis of small, piezoelectrically excited bending-wave loudspeakers," *Proceedings of Meetings on Acoustics*, 43(1), p. 030002, 2021, doi:https://doi.org/10.1121/2.0001520.

[18] Anderson, D. and Bocko, M. F., "Modal Crossover Networks for Flat-Panel Loudspeakers," *J. Audio Eng. Soc.*, 64(4), pp. 229–240, 2016, doi:http://dx.doi.org/10.17743/jaes.2016.0005.

[19] Anderson, D. A., Heilemann, M. C., and Bocko, M. F., "Measures of vibrational localization on point-driven flat-panel loudspeakers," *Proceedings of Meetings on Acoustics*, 26(1), 2016, doi: https://doi.org/10.1121/2.0000216.

[20] Rabbiolo, G., Bernhard, R., and Milner, F., "Definition of a high-frequency threshold for plates and acoustical spaces," *J. Sound Vib.*, 277(4–5), pp. 647 – 667, 2004, ISSN 0022-460X, doi: http://dx.doi.org/10.1016/j.jsv.2003.09.015.

[21] Anderson, D., Heilemann, M., and Bocko, M., "Optimal Exciter Array Placement for Flat-Panel Loudspeakers Based on a Single-Mode, Parallel-Drive Layout," in *145th Convention of the AES*, 2018, doi:https://doi.org/10.17743/aesconv.2018.978-1-942220-25-1.

[22] Fuller, C., Elliott, S., and Nelson, P., *Active Control of Vibration*, Associated Press, 1996, doi: https://doi.org/10.1016/b978-0-12-269440-0.x5000-6.

[23] Pan, J., Hansen, C. H., and Snyder, S. D., "A Study of the Response of a Simply Supported Beam to Excitation by a Piezoelectric Actuator," *J. Intell. Mater. Syst. Struct.*, 3(1), pp. 3–16, 1992, doi:https://doi.org/10.1177/1045389X9200300101.

[24] Dimitriadis, E. K., Fuller, C. R., and Rogers, C. A., "Piezoelectric Actuators for Distributed Vibration Excitation of Thin Plates," *J. Vib. Acoust.*, 113(1), pp. 100–107, 1991, doi:https://doi.org/10.1115/1.2930143.

[25] Gibbs, G. P. and Fuller, C. R., "Excitation of thin beams using asymmetric piezoelectric actuators," *J. Acoust. Soc. Am.*, 92(6), pp. 3221–3227, 1992, doi:http://dx.doi.org/10.1121/1.404172.

[26] Heilemann, M. C., *Spatial Audio Rendering with Flat-Panel Loudspeakers*, Ph.D. thesis, University of Rochester, 2018.

[27] Fuller, C., Gibbs, G., and Silcox, R., "Simultaneous Active Control of Flexural and Extensional Waves in Beams," *J. Intell. Mater. Syst. Struct.*, 1(2), pp. 235–247, 1990, doi:https://doi.org/10.1177/1045389X9000100206.

[28] Cremer, L., Heckl, M., and Petersson, B., *Structure-Borne Sound: Structural Vibrations and Sound Radiation at Audio Frequencies*, Springer Berlin Heidelberg, 2005, ISBN 9783540265146.

[29] Fahy, F. and Gardonio, P., *Sound and Structural Vibration: Radiation, Transmission and Response 2nd Edition*, Elsevier Science, 2007, ISBN 9780080471105, doi:https://doi.org/10.1016/b978-0-12-373633-8.x5000-5.

[30] Piezo Systems, "Materials Technical Data," 2022, doi:https://info.piezo.com/hubfs/Data-Sheets/piezo-material-properties-data-sheet-20201112.pdf.

[31] Mitchell, A. K. and Hazell, C. R., "A Simple Frequency Formula for Clamped Rectangular Plates," *J. Sound Vib.*, 118(2), pp. 271–281, 1987, doi: https://doi.org/10.1016/0022-460X(87)90525-6.

[32] Williams, E. G., *Fourier Acoustics*, Academic Press, London, 1999, ISBN 978-0-12-753960-7, doi:http://dx.doi.org/10.1016/B978-012753960-7/50001-2.